

Heat flux performance analysis of a generic urban environment with control volume

Berk Adali¹, Yigit Can Altan²

¹*Ozyegin University Department of Civil Engineering, İstanbul, Turkey, berk.adali@ozu.edu.tr*

²*Ozyegin University Department of Civil Engineering, İstanbul, Turkey, yigitcan.altan@ozyegin.edu.tr*

SUMMARY

Long-term projections and records indicate a change in world climate. This change will be especially observed as an increase of extreme weather frequency. Besides, the resolutions of the extreme events in the urban environment can be more severe due to the thermal properties of construction materials and the wind blockage effect of the buildings. In the scope of this study, the thermal performance of a generic urban area by specific geographical properties is simulated to quantify the adverse effects of extreme weather events in the urban environment. For this purpose, seven configurations with different physical properties (H/W, albedo level, roof type) were created using the features of the structures in the chosen area. Cases were simulated for the same weather conditions with commercial Computational Fluid Dynamics (CFD) software called ANSYS Fluent. The seven cases are compared according to the temperature at the building surfaces and heat fluxes within the generic urban area and the most suitable combination has been determined accordingly. Case VII provides the best suitable area on average surface temperature (T_s) and distribution of heat fluxes.

Keywords: Urban Heat Island (UHI), Computational Fluid Dynamics (CFD), Heat Flux

1. INTRODUCTION

Urbanization causes a change in the thermal properties of the natural earth's surface. These effects are observed as an increase in the temperature in the urban environment, called Urban Heat Island (UHI). The most significant adverse effects of UHI are observed as an increase in energy consumption for cooling purposes and a negative effect on human health. In addition to that, according to Zhao et al., (2018) heat waves increase the influence of UHI, which is another consideration for the quality of life of all livings in that region. At this point, microclimate analysis is critical for resolving these issues by quantifying the climate resolution in the first few meters above the earth's surface, where most living things are present. With the aid of the CFD analysis, these first few meters can be modeled and investigated for thermal performance. The modeling not only helps to quantify the resolution of the thermal performance but also helps to discover the causes of the adverse effects, which can be used to quantify the mitigation strategies. Mitigation solutions for the thermal performance of the urban environment can concentrate on a variety of solutions such as aspect ratio, roof design, albedo level, and convective (Q_{conv}) and turbulent (Q_{turb}) heat fluxes (Allegrini et al., 2015). The aim of this study is to compare different parameters to determine the urban model effect on the first few meters of the earth's surface with the generic

urban area. Buildings for the interest area are modeled in line with the real conditions at Yeşilköy/İstanbul. The effects of aspect ratio, albedo effect, and roof design on thermal performance are evaluated using average T_s and heat fluxes. Similar to the study of Allegrini et al., (2015), Q_{conv} and Q_{turb} are examined with the control volume created around the urban area. Unlike previous studies, the heat fluxes on the control volume surfaces are evaluated per square meter to prevent the difference due to the surface area variation. Figure 1 summarizes all the case studies.

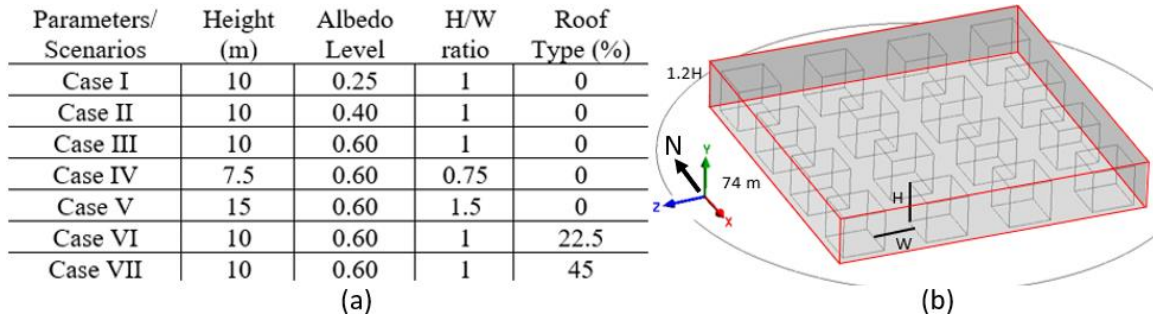


Figure 1. (a) Summary of the scenarios and (b) model geometry and control volume.

2. METHODOLOGY

The generic urban area is simulated via ANSYS Fluent. The weather conditions are taken from Turkish State Meteorological Services (TSMS) for July 29th (the warmest day of 2020 in terms of air temperature) as hourly meteorological data. To take advantage of hourly data, URANS transient simulation with realizable $k - \epsilon$ turbulence modeling is performed. The analysis of the hourly data shows that the north is the predominant wind direction, and it is used as the constant wind direction. During the simulations, logarithmic wind profile, k and ϵ are used as an input condition and calculated according to Equations (1), (2), and (3) (Toparlar et al., 2015):

$$U(z) = \frac{u^*}{\kappa} \ln\left(\frac{z+z_0}{z_0}\right) \quad (1)$$

$$k = \frac{u^{*2}}{\sqrt{C_\mu}} \quad (2)$$

$$\epsilon(z) = \frac{u^{*3}}{\kappa(z+z_0)} \quad (3)$$

Equations 1-3 represent logarithmic wind speed profile, turbulent kinetic energy, and turbulence dissipation rate, respectively. The homogenous logarithmic wind profile for the software is achieved with the wall functions. The roughness height (k_s) for the first cell is used as in Equation 4 (Blocken et al., 2007):

$$k_s = \frac{9.793 * z_0}{C_s} \quad (4)$$

The meshing is done according to best practice guidelines (Franke et al., 2007), and orthogonality ($>0,16$) and skewness ratios ($<0,5$) are achieved. Q_{conv} and Q_{turb} are determined to calculate the heat flux on surfaces of control volume that is built around the buildings (Allegrini et al., 2015) (Cengel and Ghajar, 2011):

$$Q_{conv} = \int u(T - T_{\infty})c_p\rho dA \quad (5)$$

$$Q_{turb} = \int k_{eff} \frac{\Delta T}{\Delta n} dA \quad (6)$$

In Equations (5) and (6), u is the velocity component normal to the investigated plane, T is the temperature, which is obtained from control volume, T_{∞} is the reference temperature for flow, c_p is the specific heat capacity, ρ is the density of air, k_{eff} is the effective thermal conductivity, and n is the direction normal to the plane.

3. RESULTS

Two different control mechanisms, average T_s on building surfaces, and heat fluxes on control volume are used for evaluation. First, average T_s are compared to decide on the best configuration. The hottest average T_s is seen at 11 am; therefore, it is chosen as the primary time for the upcoming investigations. At 11 am, the reference velocity speed is 2.1 m/s at 10 m above the earth's surface.

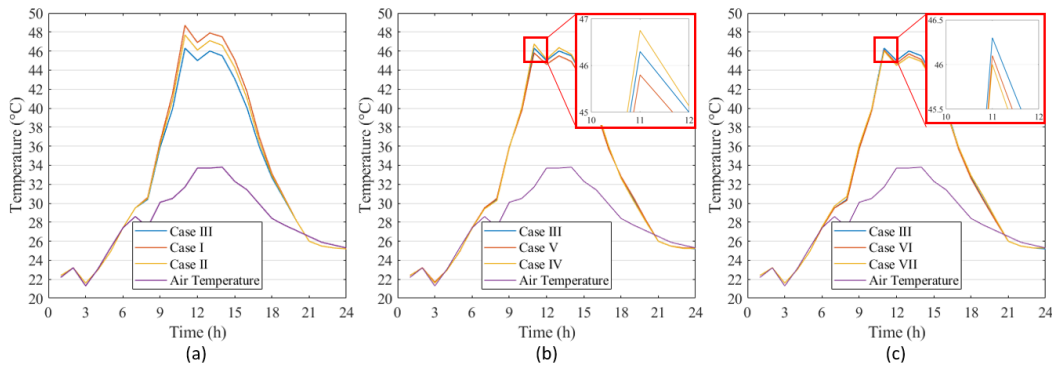


Figure 2. The average surface temperature on surfaces (a) albedo level, (b) H/W ratio, and (c) roof type.

Figure 2 shows the average T_s for all scenarios. Figure 2(a) shows that Case III has the lowest T_s due to the low absorptivity and high albedo level of the building's surface. Figure 2(b) represents the aspect ratio effect on the average T_s , and Case V has performed the best ratio in terms of T_s . An increase in the height of buildings positively affects the T_s with the increased wind speed and enhanced convective heat transfer. On the contrary, high wind speed may negatively influence people who live there according to wind pattern comfort criteria for higher wind speed conditions. Moreover, Figure 2(c) compares the results of three different roof designs. According to Figure 2(c), the roof type with a 45% slope has a higher performance in terms of the average temperature values. Overall, when all the cases are compared on average temperature and wind velocity criteria, Case VII is the best configuration due to the same average temperature as Case V, and velocity values are lower than Case III. Another control parameter is the heat flux through the surface of the control volume. It is created with different dimensions for all models to cover urban areas 2 m far away from buildings. Q_{conv} and Q_{turb} are calculated per cell, and the sum of the heat fluxes of the cells gives the total heat flux for each surface. In Figure 3(a), the Q_{conv} and Q_{turb} ratio for each surface is plotted, and it shows almost 50% of heat fluxes are emitted from the upper surface of the control volume. Notably, this ratio is affected by area differences between the four surfaces. When values are compared according to the surface areas, the upper surface area is bigger than other surfaces areas by up to 7.8 times, depending on the urban model. On the other hand, Figure 3(b) is created with heat flux per unit, and the surface area effects are eliminated. The ratio of the

heat fluxes from the upper surface decreased to 15-18.5% from 50-60% on average. While Case IV has the highest percentage of heat flux leaves from the upper surface in Figure 3(a), this ratio is decreasing, and Case VII provides the highest amount of heat flux on the upper surface in Figure 3(b). Furthermore, Figure 3 shows that even if the aspect ratio has the most impact on the heat flux ratio in Figure 3(a), when heat flux per unit is determined, changes in albedo level and aspect ratio could not affect the heat flux ratio as effectively as roof design.

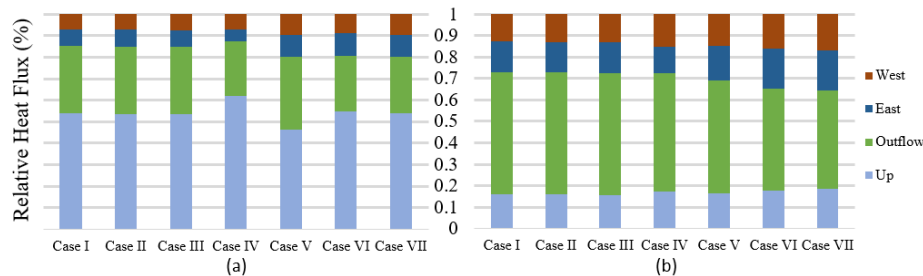


Figure 3. Relative heat fluxes with four surfaces for urban configurations, (a) Q (kW), and (b) q (kW/m²).

4. CONCLUSION

This study investigated the effects of various urban areas on average T_s and heat fluxes using CFD methods on a generic model with control volume. The location is selected as Yesilkoy/Istanbul, and the weather conditions of July 29th (2020) are simulated. Average T_s , wind speed, and heat flux distributions are used as evaluation criteria. Considering these observations, it is seen that examining the heat flux as per m² gives a more successful result than the total heat flux. Also, Case VII found the best configuration on average T_s , wind speed, and heat flux distribution. As a future work, the determination of the economic effects of these parameters can be investigated to evaluate the positive impact. In addition, to make a clear comparison of each model, areas of inflow surface ratio comparison for the cases can be calculated to create a relationship between the cases.

REFERENCES

- Allegrini, Jonas, Viktor Dorer, and Jan Carmeliet. 2015. "Coupled CFD, Radiation and Building Energy Model for Studying Heat Fluxes in an Urban Environment with Generic Building Configurations." *Sustainable Cities and Society* 19: 385–94. <https://doi.org/10.1016/j.scs.2015.07.009>.
- Blocken, Bert, Ted Stathopoulos, and Jan Carmeliet. 2007. "CFD Simulation of the Atmospheric Boundary Layer: Wall Function Problems." *Atmospheric Environment* 41 (2): 238–52. <https://doi.org/10.1016/j.atmosenv.2006.08.019>.
- Cengel, Yunus A, and A Ghajar. 2011. "Heat and Mass Transfer (a Practical Approach, SI Version)." *McGraw-670 Hill Education* 671: 52.
- Franke, Jörg, Antti Hellsten, Heinke Schlünzen, Bertrand Carissimo, Alexander Baklanov, Photios Barmpas, and John Bartzis. 2007. *Best Practice Guideline for the CFD Simulation of Flows in the Urban Environment: COST Action 732 Quality Assurance and Improvement of Microscale Meteorological Models Enviro-RISKS: Man-Induced Environmental Risks: Monitoring, Management and Remediation O*. <https://research.aalto.fi/en/publications/best-practice-guideline-for-the-cfd-simulation-of-flows-in-the-ur>.
- Toparlar, Y., B. Blocken, P. Vos, G. J.F. Van Heijst, W. D. Janssen, T. van Hooff, H. Montazeri, and H. J.P. Timmermans. 2015. "CFD Simulation and Validation of Urban Microclimate: A Case Study for Bergpolder Zuid, Rotterdam." *Building and Environment* 83: 79–90. <https://doi.org/10.1016/j.buildenv.2014.08.004>.
- Zhao, Lei, Michael Oppenheimer, Qing Zhu, Jane W. Baldwin, Kristie L. Ebi, Elie Bou-Zeid, Kaiyu Guan, and Xu Liu. 2018. "Interactions between Urban Heat Islands and Heat Waves." *Environmental Research Letters* 13 (3). <https://doi.org/10.1088/1748-9326/aa9f73>.